EDFAAO (2025) 1:18-25

1537-0755/$19.00

QUANTUM DIAMOND MICROSCOPY FOR SEMICONDUCTOR FAILURE ANALYSIS

Marwa Garsi, Andreas Welscher, Manuel Schrimpf, Bartu Bisgin, Michael Hanke, Horst Gieser, Daniela Zahn, and Fleming Bruckmaier
QuantumDiamonds, Munich, Germany
marwa.garsi@quantumdiamonds.de

INTRODUCTION

As heterogeneous integration (HI) and advanced packaging become increasingly prevalent for achieving the next wave of performance improvements, conventional electrical failure analysis (EFA) techniques are facing growing challenges in meeting industry demands.[1,2] Emerging trends like wafer-to-wafer and chip-to-wafer bonding, through-silicon vias, and backside power delivery are significantly increasing interconnect complexity. Because interconnects are critical to the performance gains in state-of-the-art devices, ensuring their electrical integrity is crucial for ramping up production and maintaining high yields. However, many traditional EFA techniques struggle to cope with weak signals, multiple metallization layers, and stacked dies. Moreover, the increasing adoption of wide band-gap materials such as GaN and SiC results in further complications in current EFA.[3] There is a dire need for new methods that can localize faults that are deep below the surface and surrounded by complex metallization, with three-dimensional information, high resolution, and short measurement times.

One of the emerging EFA techniques addressing these problems is quantum sensing with nitrogen-vacancy (NV) centers in diamond.[4,5] The technique enables magnetic field measurements with high spatial resolution and sensitivity, allowing the user to image the electrical activity within the circuit and identify various failure modes, including shorts and opens. This process is known as magnetic current imaging (MCI).[6,7] Because magnetic fields travel through Si, GaN, and SiC unimpeded, this modality is a promising candidate for identifying buried and weak failures within the deep layers, as well as new power devices. Furthermore, compared to other magnetic current imaging techniques such as SQUIDs, this technique achieves higher resolution, does not require scanning, and operates at room conditions, making it appealing from a practical EFA standpoint. A system that performs quantum sensing using diamonds has colloquially come to be known as a quantum diamond microscope (QDM).

This article presents the QDM as an innovative FA tool, details its operation from an FA engineer's perspective, and discusses its place in the overall FA workflow. The focus then turns to the lateral resolution metric and analysis of two different integrated circuits: a simple Cu wire test sample, and a commercially available quadrupole NAND-gate circuit (Texas Instruments, CD4011-B). Both samples were selected to familiarize the FA engineer with magnetic field and current density data and are ideal to demonstrate the technique, due to their easy-to-understand layouts. Here, a lateral magnetic resolution of 3.0(5) µm is showcased, which is already competitive for EFA.[2] The article concludes by comparing QDM to existing EFA methods in terms of relevant metrics, such as resolution and measurement time.

QDM FOR FAILURE ANALYSIS

Currents flowing through conductive paths in integrated circuits (ICs) generate localized magnetic fields, as described by Ampère's law.[8] Mapping these fields provides crucial insights into current-density distribution, allowing for the identification and localization of circuit anomalies. However, previous MCI methods, such as SQUIDs and GMR sensors, have faced limitations due to impractical system requirements and a steep trade-off between resolution, sensitivity, and acquisition times caused by scanning-mode systems.

Quantum sensing using a QDM addresses these challenges by enabling MCI with high spatial resolution,

room-temperature operation, and fast acquisition times, enhancing the FA workflow. A key advantage of the QDM is its ability to capture the complete vectorial magnetic field, enabling a detection of vertical currents, while other MCI systems measure only a single projected field component. The QDM can map magnetic fields from multiple layers of the device-under-test (DUT), including vertical interconnects, and create detailed images of electrical activity. Analysis of these images allows FA engineers to localize faults such as shorts and opens, providing valuable insights for root-cause analysis.

The QDM achieves MCI by combining advanced microscopy optics with a diamond quantum sensor to transduce the magnetic field into an optical signal, transducing the magnetic field into an optical signal that is captured by a camera as a spatially resolved image. A generic testing setup is shown in Fig. 1. For more information on QDM working principles and the underlying physics, the reader is encouraged to consult the comprehensive report in reference 9.

PERFORMANCE PARAMETERS OF THE QDM

Several factors are crucial for the FA engineer for failure localization in the HI era: depth reach, sensitivity, and resolution. Depth reach can be functionally understood as the maximum distance at which a signal can be meaningfully detected. Sensitivity defines the minimum detectable magnetic field strength within a given time window and is closely linked to the minimum detectable current. Because the QDM can generate x, y, and z coordinates, two parameters are important to evaluate: lateral and depth resolution.

Similar to conventional optical FA techniques, the resolution is strongly dependent on the depth of the current or feature under investigation. Typical lateral resolutions achieved under laboratory conditions are on the order of ~ 0.5-5 µm for surface-level currents. Having a depth resolution is a discerning factor compared to most optical techniques such as photo-emission microscopy (PEM), optically induced resistance change (OBIRCH), and thermally induced voltage alteration (TIVA, also referred to as infrared OBIRCH), which has no depth sensing capabilities beyond shallow defects.[10,11] Lock-in thermography (LIT) is the exception and does supply depth information.[12] However, its depth accuracy depends on precise knowledge of thermal properties of the materials involved, which is usually not straightforward. While the depth resolution of QDM can also strongly depend on the given sample, typically achieved uncertainties of a given

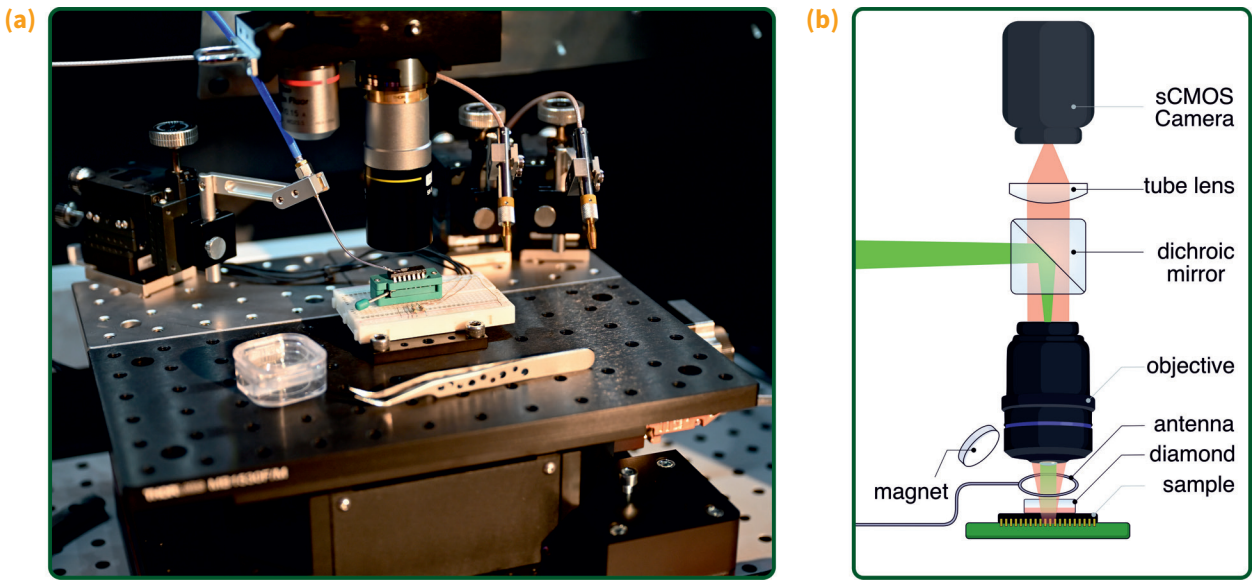

Fig. 1 **(a) Stage of a QDM system. A breadboard with a zero-insertion force socketed sample is positioned beneath an objective, alongside additional probe needles. (b) Illustration of a QDM setup. A 532 nm green laser is directed to a dichroic mirror and then into an objective, after which the laser beam is collimated. The laser illuminates the diamond quantum sensor placed on top of the IC sample, causing the NV centers within the diamond to fluoresce. The intensity of the NV centers' fluorescence depends on both the microwave frequency, which is swept by the nearby antenna, as well as the local magnetic field. The active die's currents alter these local magnetic fields with respect to the bias field, leading to variations in the fluorescence intensity across the field of view (FoV). The resulting red fluorescence passes back through the objective, continues through the dichroic mirror, and is then collected by a camera. The fluorescence intensity, recorded to each pixel, encodes detailed information about the sample's local magnetic fields, enabling the extraction and imaging of integrated circuit activity.**

depth is 10%. As an example, the depth uncertainty of a current-carrying wire 50 µm below the surface where the sensor is placed, would be ~ 5 µm.

OPERATION OF A QDM FROM THE FA ENGINEER'S PERSPECTIVE

Operation of a QDM involves a two-step process:

Step 1: The DUT must be prepared within the biasing conditions. Secondly, the sensor positioning must take place. The interaction of the DUT with the quantum sensor can be achieved in two main ways. Either the quantum sensor is a stand-alone diamond chip and is placed directly on the sample, or it is integrated into the microscope objective and is brought close to the sample. In the stand-alone case (as illustrated in Fig. 1b), the sensor can directly be placed on top of the region of interest on the DUT. The diamond is in contact with one side of the sample, therefore achieving a minimal stand-off distance to the area of interest (limited by the flatness of the sample surface). Note that despite being placed on the surface, the sensor collects information through the layers of the DUT. As an example, a QDM that uses the stand-alone sensor configuration and has a sensitivity of ~ 5 $\mu T(Hz)^{-0.5}$ will be able to image currents of ~ 1 mA buried at a distance of up to ~ 300 µm with a reasonable signal to noise ratio of 3 within ~20 seconds. In the case of diamond sensors integrated into the optical setup,[13] automation is essential for aligning the sensor with the region of interest, while tilt correction should ensure flatness. The depth reach and resolution of the integrated sensor will diminish as the distance between the objective head and the sample increases.

Generally, the diamond sensors are usually cuboid chips with sides of length 1-4 mm, which allows to image a FoV up to 4 mm x 4 mm. The stand-alone case is appealing when samples have rough and hard-to-reach surfaces (typical for wide band-gap devices such as GaN), because the objective can be moved farther from the sample stage, while the integrated case is appealing when samples are flat and automation is desired, e.g. when stitching data over a wafer.

Step 2: After sensor positioning is done, the measurement is automated and requires no interference from the operator. Magnetic field maps are created, and the source current density images are extracted. The operator can use infrared (IR) backside images and their knowledge of the layout (if available) to precisely pinpoint current paths in either a single or multiple layers.

QDM IN THE FA WORKFLOW

As an MCI method, the QDM can identify all failures addressable by traditional MCI techniques while also overcoming certain prior limitations.[7] Generally, the addressable faults include shorts, leakages, and high-resistance faults. However, the QDM can also identify true non-resistive opens using AC-currents on the DUT, which remained a challenge for many imaging methods to this date.[1] Table 1 gives a summary of addressable failure modes.

QDM is a versatile tool that can be incorporated into the FA workflow in two different points. First, it can be used as a nondestructive inspection tool before sample preparation. This could either be over-the-package or after decapsulation without thinning and polishing. It is generic to use LIT for this step in FA labs that have access to such a device. Here, QDM can be seen as a supplement to the hotspot information, but also has the potential to surpass the depth detection and resolution capabilities of LIT. These prospects are actively being investigated.

Table 1 List of addressable failures for packages and dies for QDM.

Package-level	Package high-R	Die-level	Die high-R
Shorts, leakages, opens	Bumping voids C4 and µ-bumps, vias	Power shorts, IDD leakage, I/O leakage	Upper metal defects

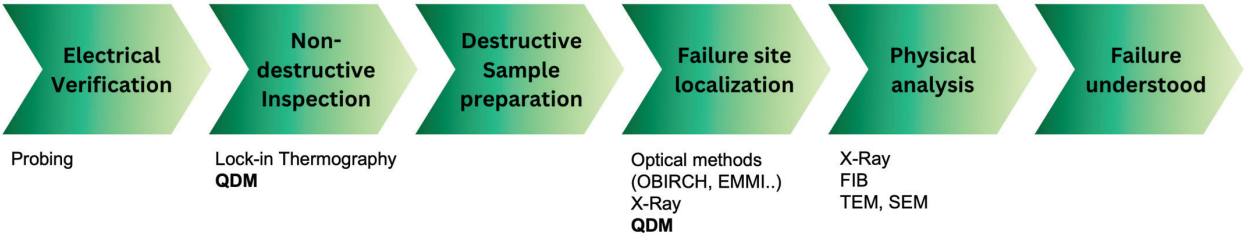

Fig. 2 **Flowchart of a generic FA workflow. Steps 2 and 4 are value-proposition points for QDM as a versatile tool that can be used both before and after sample preparation, with different benefits: nondestructive overview and very high lateral resolution, respectively.**

Second, the QDM can also be used after the sample preparation, where molding has been taken off and the die is exposed and thinned down. This is where previously mentioned methods such as EMMI, OBIRCH, as well as x-ray methods would be commonly used. Here QDM excels at providing µm resolution images in a short amount of time, as well as providing direct information about electrical activity in the form of an image. Another benefit of QDM is that it does not require sample polishing, even for highly doped samples, which decreases the overall time spent on sample preparation. Due to its depth sensing capabilities, the QDM can also identify a defective layer much earlier than many optical methods, saving the FA engineer hours of layer-by-layer thinning. Figure 2 illustrates QDM's place in the FA workflow.

This article focuses on demonstrating QDM's capabilities for lateral resolution on two different samples and familiarizing the reader with the magnetic and current density measurement data. QDM's capabilities of depth reach, depth resolution, and sensitivity will be analyzed in a later work.

SPATIAL RESOLUTION OF THE QUANTUM DIAMOND MICROSCOPE

Several factors influence the spatial resolution of magnetic field images, defining the accuracy with which magnetic phenomena can be mapped in integrated circuits. The optical spatial resolution of the system described in this article sets the lower limit and depends on the numerical aperture (NA) of the optical system. To achieve maximum resolution, diamond solid immersion lenses are available achieving up to 200 nm optical resolution. The primary limiting factor, however, is the standoff distance—the gap between the NV centers and the electronic circuit under test. This distance influences resolution due to the decay of magnetic field strength with increasing distance. Notably, while the standoff distance affects spatial resolution, it also offers valuable insights into the depth of the current under investigation.

To demonstrate the spatial resolution of this system, the team acquired vectorial magnetic field images of a current-carrying wire sample, provided by Hamamatsu's PHEMOS group. The measurement results using QDM are shown in Fig. 3a. The experimental setup included an infinity-corrected objective with 50x magnification and a numerical aperture (NA) of 0.55, optimizing the system for a balance between field depth and resolution. The sample, a 500 nm thick wire, carried a current of 1 mA, generating magnetic fields on the order of 50 µT, which were mapped across a predefined area as the current flowed through the wire's path.

As discussed in reference 14, there are multiple ways to define the spatial resolution of the MCI. Here, spatial resolution is defined as the ability to resolve contribution from two parallel current paths as described by Sparrow's criterium.[15] By taking a line cut along the x-axis of the signal generated by a single wire where current flows in the y-direction, the spatial resolution can be estimated as the 15-85 % raise of the signal. B_z signals have a different behavior, and the peak-to-peak distance is a definition generally adopted since it is easy to identify. Looking at the B_x profile gives a spatial resolution of 3.0(5) µm.

Analyzing the magnetic field profiles generated by a current-carrying wire shows that B_x and B_z components exhibit distinct spatial behaviors. The B_x field has a more confined profile with a sharper peak, whereas the B_z field tends to display broad lateral extensions, resulting in a more gradual decay at greater distances from the wire.

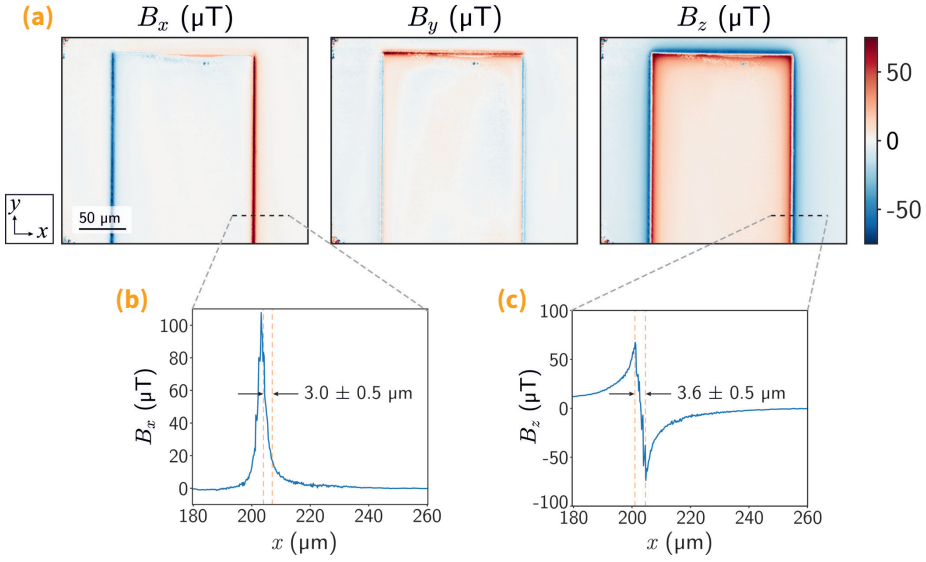

Fig. 3 Magnetic field images of a 1 mA current-carrying wire, used to determine the magnetic resolution. (a) Amplitudes of B_x, B_y, and B_z magnetic field components, where a positive B_x value indicates an upward current and a positive B_y value indicates a right-to-left current. (b) Line cut of B_x along the x-axis, indicated in (a) by a dashed black line. The resolution is determined using Sparrow's criterion, with 15% and 85% of the total magnetic magnitude shown by dashed orange lines. (c) Line cut of B_z along the x-axis, also marked in (a) by a dashed black line. Resolution is determined by the peak-to-peak distance, indicated by dashed orange lines.

These broad extensions lead to the long-range behavior of the B_z field.

Due to the broader distribution of the B_z field, spatial resolution is less precise when using B_z for localizing sources. In contrast, the B_x field shows a sharper transition, with a steeper slope around the wire, making it more sensitive to small changes in position. This leads to better spatial resolution, allowing for more accurate identification of the wire's position and the distance over which the field changes.

Thus, for identifying current-carrying features or mapping magnetic fields over small areas, the B_x profiles offer a significant advantage over B_z, which tends to blur finer spatial details due to its broad lateral extensions. This makes the QDM particularly advantageous in such applications, especially for higher stand-off distances where spatial broadening can become critical.

Finally, it is important to note that the thickness of the sensor plays a role. Therefore, different diamonds with different properties can be designed for specific use cases, such as die-level or package-level analysis. Further careful system design and calibration can push these boundaries, allowing for more detailed and accurate mapping of magnetic fields in semiconductor devices.

CURRENT PATH MAPPING IN NAND GATES

NAND gates are a fundamental building block of digital logic in CMOS technology. This section investigates the current paths in the Texas Instruments CD4011B, a quad NAND gate IC shown in Fig. 4 with a publicly available layout.

Table 2 presents the truth table for a NAND gate. A logical '0' corresponds to a low voltage relative to ground, while a logical '1' indicates a high voltage. A consistent high state of 5 V was applied to the gate inputs, with the output connected to ground through a 10 kΩ resistor.

Table 2 Truth table for a NAND gate, where A and B represent the inputs, and the third column is the resulting output.

A	B	NAND (A, B)
0	0	1
0	1	1
1	0	1
1	1	0

Each NAND gate comprises two input pins and one output pin. Contact Pins 1 and 2 function as the inputs for the first NAND gate, with Contact Pin 3 serving as the output. This configuration is repeated for the other three NAND gates. Pin 7 is grounded, while Pin 14 serves as the voltage supply (VDD). Magnetic field signatures generated by operating currents under various input configurations were measured using the QDM. Figure 5 illustrates the resulting magnetic fields obtained with a supply current of 8 mA and all input gates set to '0' (i.e., in a low state).

The magnetic field maps already contain all the necessary information to localize failures or track current, however, they can be challenging to interpret for the FA engineer, especially for complex chip configurations. To this end, current reconstruction procedures enable reconstructing the current density.[16-18] Using machine learning approaches, allows retrieving the current density path using the magnetic field maps as input data. Figure 6 shows current densities for two distinct gate configurations.

Demonstrating the ability to image currents with different gate configurations, establishes the capability to track current paths through ICs. This functionality enables FA engineers to precisely locate areas of anomalous behavior, such as leakage currents, shorts, or open circuits, which are often challenging to detect using traditional methods. Thus, visualizing current flow allows engineers to better understand the nature and location of faults, resulting in

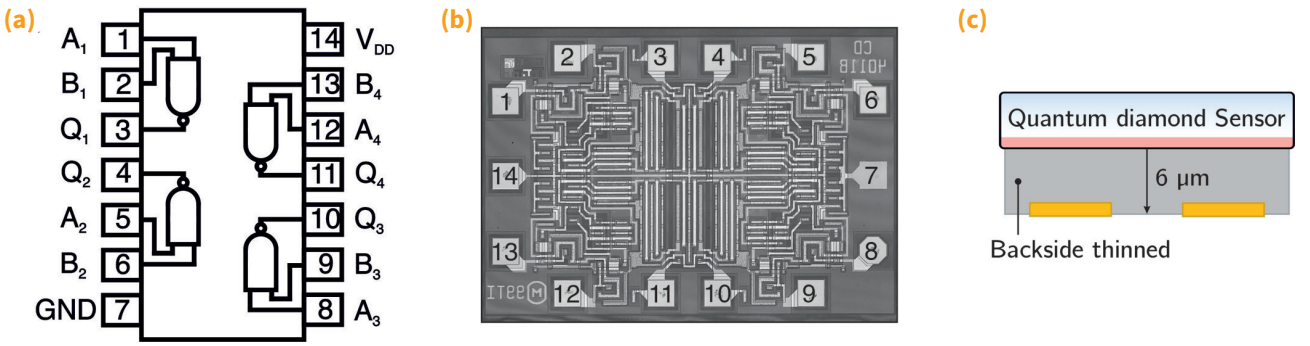

Fig. 4 (a) Layout and (b) infrared image of the Texas Instruments CD4011B IC with four NAND gates. (c) Cross-section illustrating the stand-off distance between the sample to probe and the diamond sensor.

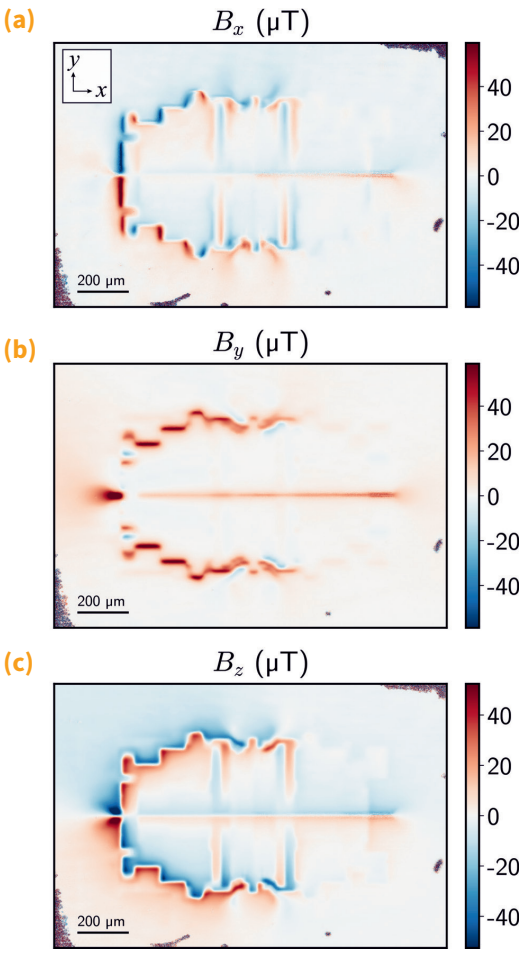

Fig. 5 Magnetic field maps of CD4011B activity acquired using the QDM. A current of 8 mA was applied to power the chip. (a) The B_x component arises from currents flowing along the y-axis, where positive values indicate upward currents, and negative values represent downward currents. (b) The B_y component corresponds to currents along the x-axis, with positive values indicating right-to-left currents, and negative values indicating left-to-right currents. (c) The B_z component represents the out-of-plane magnetic field, encompassing contributions from currents along both the x- and y-axes.

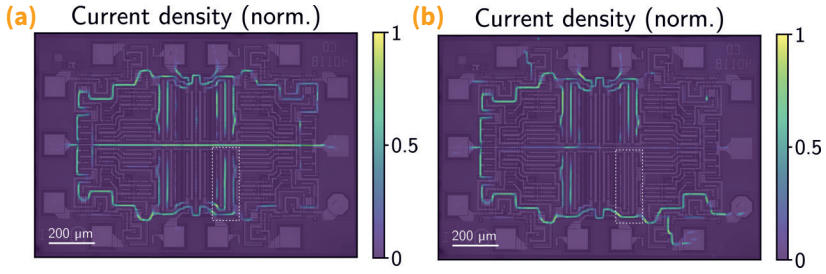

Fig. 6 Overlay of the current density for various input combinations of the controllable NAND gates with the IR image of the IC. (a) Current reconstructed from magnetic field measurements, with all input gates set to a low state. (b) Current reconstructed from magnetic field measurements, where both input gates, Pins 8 and 9 of the lower-right NAND gate were in a high state, resulting in an absence of current in the highlighted (dotted) area.

more accurate diagnosis and efficient problem-solving. This leads to reduced debugging time, improved reliability, and more effective root-cause analysis, particularly in complex circuits.

The next step for the QDM's application in EFA is to assess its ability to map current paths within more advanced multi-layered chips, particularly those involved in heterogeneous integration. By further enhancing depth sensitivity and improving spatial resolution, QDM technology is poised to become an indispensable tool in the analysis of complex semiconductor devices, providing critical insight into both lateral and vertical current flows.

CONCLUSION AND OUTLOOK

This article introduced quantum sensing with diamond through the QDM as an innovative, nondestructive EFA tool. Detailed operation from an FA engineer's perspective shows how it integrates into standard workflows. Measurements on two integrated circuits demonstrated a lateral spatial resolution of 3.0(5) µm, illustrating the type of data a QDM provides. Its performance was compared to established FA methods, highlighting its specific advantages.

Although the QDM is still in its early development stages, akin to the adoption of lock-in thermography in the 2000s, initial results reveal strong application potential. There are several ways to improve the QDM; for example, transitioning to AC imaging could leverage NV sensors' established sensitivities in the nT to pT (Hz)-0.5 range at MHz and GHz frequencies,[19] potentially accelerating measurements by several orders of magnitude and enabling assessments of ICs at their native clock frequencies.

In conclusion, the QDM shows considerable promise as an FA tool, particularly as the field advances toward heterogeneous integration and wide band-gap materials. Future work will focus on over-the-package analysis with a QDM, aiming to establish its depth-sensing capabilities.

ACKNOWLEDGMENTS

The authors would like to thank the PHEMOS team of Hamamatsu Photonics for fruitful discussions and providing the copper wire sample shown in Fig. 2. They would also like to thank Prof. Dominik Bucher and Robin Allert for discussions on this subject.

REFERENCES

1. IEEE International Roadmap for Devices and Systems, Metrology, Institute of Electrical and Electronics Engineers, 2023.

2. N. Antoniou and B. Foran: "The EDFAS FA Technology Roadmap—FA Future Roadmap," *EDFA,* May 2023, *25*(2), p. 44-46, doi.org/10.31399/asm.edfa.2023-2.p044.
3. M. Mullen: "Wide Bandgap – Semiconductor Failure Analysis – Illuminating Semiconductors," 2024, thermofisher.com/blog/semiconductors/failure-analysis-of-wide-bandgap-semiconductor-devices.
4. P. Kehayias, et al.: "High-Resolution Short-Circuit Fault Localization in a Multilayer Integrated Circuit using a Quantum Diamond Microscope," *Phys Rev Appl,* 2023, *20,* p. 014036.
5. M. Garsi, et al.: "Three-dimensional Imaging of Integrated-circuit Activity using Quantum Defects in Diamond, *Phys Rev Appl,* 2024, *21,* p. 014055.
6. L.A. Knauss: "Magnetic Field Imaging using a SQUID for Fault Isolation," *EDFA,* May 2000, *2*(2), p. 1-10, doi.org/10.31399/asm.edfa.2000-2.p001.
7. A. Orozco: "Magnetic Current Imaging in Failure Analysis," *EDFA,* November 2009, *11*(4), p. 14-21, doi.org/10.31399/asm.edfa.2009-4.p014.
8. R.H. Good and T.J. Nelson: "Classical Theory of Electric and Magnetic Fields," Academic Press, 1974.
9. E.V. Levine: "Principles and Techniques of the Quantum Diamond Microscope," *Nanophotonics,* 2019, *8,* p. 1945-1973.
10. K. Nikawa: "Optical Beam Induced Resistance Change (OBIRCH): Overview and Recent Results," 2003, p. 742-743, doi.org/10.1109/LEOS.2003.1253014.
11. K. Nikawa, et al.: "Failure Analysis Case Studies using the IR-OBIRCH (Infrared Optical Beam Induced Resistance Change) Method," *Proceedings of the Asian Test Symposium,* 1999, p. 394-399.
12. O. Breitenstein, et al.: "Thermal Failure Analysis by IR Lock-in Thermography," 2011.
13. G.J. Abrahams, et al.: "An Integrated Widefield Probe for Practical Diamond Nitrogen-vacancy Microscopy," *Appl Phys Lett,* 2021, *119,* p. 254002.
14. B.D. Schrag, et al.: "Magnetic Current Imaging with Magnetic Tunnel Junction Sensors: Case Study and Analysis, 2005.
15. K. Chang, et al.: "Nanoscale Imaging of Current Density with a Single-Spin Magnetometer," *Nano Lett,* 2017, *17,* p. 2367-2373.
16. B.J. Roth, N.G. Sepulveda, and J.P. Wikswo: "Using a Magnetometer to Image a Two-dimensional Current Distribution," *J Appl Phys,* 1989, *65,* p. 361-372.
17. D.A. Broadway, et al.: "Improved Current Density and Magnetization Reconstruction through Vector Magnetic Field Measurements," *Phys Rev Appl,* 2020, *14,* p. 024076.
18. N.R. Reed, et al.: "Machine Learning for Improved Current Density Reconstruction from 2D Vector Magnetic Images," 2024, https://arxiv.org/abs/2407.14553v1.
19. J.F. Barry, et al.: "Sensitive ac and dc Magnetometry with Nitrogen-vacancy-center Ensembles in Diamond," *Phys Rev Appl,* 2024, *22,* p. 044069.

ABOUT THE AUTHORS

Marwa Garsi holds a Ph.D. in quantum technologies from the Technical University of Stuttgart, where she pioneered foundational work in NV-based imaging for semiconductor electrical fault analysis. She leads the hardware development department at QuantumDiamonds.

Andreas Welscher holds a M.Sc. in physics from the Technical University of Munich and works at QuantumDiamonds. He has extensive experience in performing NV-based failure analysis tests and has performed all the measurements presented in this paper.

Manuel Schrimpf holds a M.Sc. in chemistry from the Technical University of Munich. He performed magnetic field data analyses at QuantumDiamonds and has played a pivotal role in developing the analytical code used in the presented work.

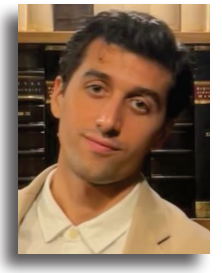

Bartu Bisgin holds a joint M.Sc. in quantum science and technology from the Technical University of Munich and Ludwig-Maximilian University. He works at QuantumDiamonds as a project manager in the failure analysis market. He has expertise in design, nanofabrication, and testing of integrated photonics.

Michael Hanke has a Ph.D. in physics from RKU Heidelberg. He has multiple years of experience in developing machine learning models and data analysis tools for spectroscopy, signal processing, and optical hardware from his work at BASF group. Currently he is spearheading software development at QuantumDiamonds and has significantly contributed to the data processing shown in this work.

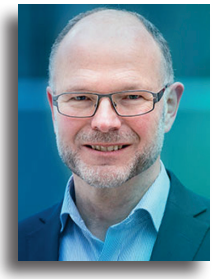

Horst A. Gieser holds a Ph.D. from the Technical University of Munich in electrical and electronics engineering. He currently leads the analysis and test department at Fraunhofer EMFT, where he oversees pioneering efforts in microelectronics and sensor systems.

ABOUT THE AUTHORS (cont'd)

Daniela Zahn holds a Ph.D. from the Fritz Haber Institute of the Max Planck Society (FHI). She is a senior researcher at Fraunhofer EMFT, specializing in quantum sensing and quantum computing applications. She is engaged in collaborative projects within the Munich Quantum Valley network, with a particular focus on the development of high-resolution microscopes for semiconductor analysis and the optimization of superconducting qubits.

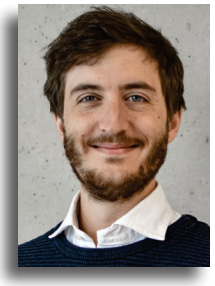

Fleming Bruckmaier holds a Ph.D. in quantum technologies from the Technical University of Munich and has over seven years of experience working in quantum sensing and imaging. His research has resulted in numerous high-ranking publications, particularly in the field of magnetic field imaging using quantum technologies, with applications in both the semiconductor and medical sectors. He serves as CTO of QuantumDiamonds, spearheading the technical development of NV-based semiconductor EFA.